Cellular and Molecular Life Sciences (2025) 82:159
https://doi.org/10.1007/s00018-025-05688-8

ORIGINAL ARTICLE

SGLT2 inhibitor empagliflozin ameliorates tubulointerstitial fibrosis in DKD by downregulating renal tubular PKM2

Xiang Cai[1,2,3,4] · Huanyi Cao[2,5] · Meijun Wang[1,2,6] · Piaojian Yu[1,2,3,4] · Xiaoqi Liang[7] · Hua Liang[8] · Fen Xu[1,2,3,4] · Mengyin Cai[1,2,3,4]

Received: 2 December 2024 / Revised: 28 March 2025 / Accepted: 1 April 2025

Abstract

Background and objective Sodium-glucose cotransporter 2 (SGLT2) inhibitors have been shown to prevent the progression of diabetic kidney disease (DKD). However, their impact on renal fibrosis remains largely uninvestigated. This study aimed to explore the effect of SGLT2 inhibitor empagliflozin on renal fibrosis in DKD patients and DKD models, and the molecular mechanisms involved.

Methods Kidney samples of DKD patients and DKD models were used in this study. DKD mouse models included STZ-treated CD-1 mice and HFD-fed C57BL/6 mice were all treated with empagliflozin for 6 to 12 weeks. Kidney pathological changes were analysed and fibrotic factors were detected. HK-2 cells were treated with normal glucose (NG), high glucose (HG), or HG with empagliflozin. RNA sequencing was employed to identify the differentially expressed genes. Epithelial–mesenchymal transition (EMT) markers were detected. Binding of transcription factor and target gene was determined using a dual-luciferase reporter assay.

Results Empagliflozin significantly ameliorated kidney fibrosis in DKD patients and DKD models. This was evidenced by tubulointerstitial fibrosis reduction observed through PAS and Masson staining, along with fibrotic factors downregulation. RNA sequencing and the subsequent in vitro and in vivo validation identified PKM2 as the most significantly upregulated glycolytic enzyme in DKD patients and models. Empagliflozin downregulated PKM2 and alleviated EMT and renal fibrosis. Importantly, empagliflozin improves fibrosis by downregulating PKM2. The downregulation of PKM2 by empagliflozin was achieved by inhibiting the binding of estrogen-related receptor α at the promoter.

Conclusions Empagliflozin ameliorates kidney fibrosis via downregulating PKM2 in DKD.

Keywords Diabetic kidney disease · Epithelial-to-mesenchymal transition · Pyruvate kinase M2 · Sodium-glucose cotransporter 2 inhibition · Tubulointerstitial fibrosis

✉ Fen Xu
xufen3@mail.sysu.edu.cn

✉ Mengyin Cai
caimengyin@mail.sysu.edu.cn

1 Department of Endocrinology and Metabolism, Third Affiliated Hospital of Sun Yat-Sen University, No. 600, Tian He Road, Tian He District, Guangzhou 510630, Guangdong, People's Republic of China

2 Guangdong Provincial Key Laboratory of Diabetology, The Third Affiliated Hospital of Sun Yat-Sen University, Guangzhou, Guangdong, People's Republic of China

3 Guangzhou Municipal Key Laboratory of Mechanistic and Translational Obesity Research, The Third Affiliated Hospital of Sun Yat-Sen University, Guangzhou, Guangdong, People's Republic of China

4 Medical Center for Comprehensive Weight Control, The Third Affiliated Hospital of Sun Yat-Sen University, Guangzhou, Guangdong, People's Republic of China

5 Department of Endocrinology, Guangdong Provincial People's Hospital, Guangdong Academy of Medical Sciences, Guangzhou 510080, People's Republic of China

6 Xunfei Healthcare Technology Co., Ltd., Hefei, People's Republic of China

7 Department of Animal Experimental Center, the Third Affiliated Hospital of Sun Yat-Sen University, Guangzhou, People's Republic of China

8 Department of Endocrinology and Metabolism, Shunde Hospital of Southern Medical University (The First People's Hospital of Shunde), Foshan, People's Republic of China

Published online: 16 April 2025

Introduction

Diabetic kidney disease (DKD), one of the most prevalent complications of diabetes mellitus, is a leading cause for end-stage renal disease and increasingly aggravate the significant global burden [1]. Renal fibrosis is a key characteristic of DKD. The development of renal fibrosis has been shown to cause the progress of renal function decline and serves as a common result to renal failure.

SGLT2 inhibitors have been recommended in the American Diabetes Association guidelines for chronic kidney disease treatment in diabetic patients [2, 3]. Large clinical trials have shown that SGLT2 inhibitors significantly slow the progression to renal failure in patients with DKD [4–8]. However, these trials primarily focus on parameters such as blood creatinine levels, estimated glomerular filtration rate (eGFR), and urine albumin-to-creatinine ratio (UACR), which are more indicative of glomerular injury rather than renal fibrosis, an important cause of renal failure. Moreover, in both clinical and preclinical studies, SGLT2 inhibitors have been reported to modulate multiple pathways implicated in renal fibrosis among patients with diabetic kidney disease (DKD). Canagliflozin has been reported to downregulate plasma levels of inflammatory markers, including TNF receptor 1, IL-6, matrix metalloproteinase 7, and fibronectin 1, in patients with diabetic kidney disease [9]. SGLT2 inhibitors also reduce DNA oxidation and activate antioxidant mechanisms in diabetic patients, indicating their role in anti-oxidation and the maintenance of cellular redox homeostasis in diabetic kidney disease (DKD) patients [10–12]. Additionally, SGLT2 inhibitors have been observed to reduce renal macrophage infiltration in DKD mouse models and in type 2 diabetic patients at high cardiovascular risk [13, 14]. Given the significant effects of SGLT2 inhibitors on improving DKD and the critical role of renal fibrosis in driving the progression of DKD, it is essential to continue exploring the specific molecular mechanisms through which these drugs ameliorate renal fibrosis, which will aid in identifying additional therapeutic targets for DKD. Consequently, extensive pre-clinical and clinical studies are still required to investigate the anti-fibrotic effects of SGLT2 inhibitors.

SGLT2 inhibitors directly target renal tubular proximal cells (RTPCs) in DKD. Importantly, during the development of renal fibrosis, proximal renal tubule is the epicenter [15, 16]. RTPCs are not only affected members of the injury, but also active promoters. Renal tubular epithelial cells can promote renal fibrosis through multiple mechanisms. Epithelial-to-mesenchymal transition (EMT) is critical for the development of renal interstitial fibrosis [17]. EMT is characterized by a loss of epithelial phenotype and a gain of profibrotic features [18, 19]. Upon activation of EMT, RTPCs undergo a transition where they lose their epithelial markers, leading to collagen deposition and renal fibrosis. In addition to EMT, damaged tubules produce and release bioactive molecules that recruit inflammatory cells, thereby activating myofibroblast differentiation, proliferation, and matrix secretion [20]. Moreover, G2/M phase cell cycle arrest and apoptosis of tubular epithelial cells can promote renal fibrosis by activating the JNK signaling pathway, which leads to the upregulation of profibrotic factors, stimulation of fibroblast proliferation, and accumulation of extracellular matrix [21, 22]. Therefore, it is crucial to explore the impact of SGLT2 inhibitors on RTPCs in DKD-related renal fibrosis, as well as the underlying molecular mechanisms involved.

In the present study, we examined the effect of empagliflozin, an SGLT2 inhibitor on ameliorating kidney fibrosis in patients with DKD and in DKD models, while also investigating the underlying molecular mechanism.

Materials and methods

Human samples

Diabetic patients were diagnosed with DKD by kidney biopsy. The human biopsy samples from DKD patients were obtained from puncture specimens. The patients were divided into two groups: one group did not receive SGLT2 inhibitors (SGLT2is), while the other group were treated with SGLT2is. All patients included in this study received the maximum tolerated dose of angiotensin-converting enzyme inhibitor/angiotensin-receptor blocker. The exclusion criteria were as follows: age < 18 years; the presence of other types of kidney disease; pregnancy; infection; genetic disease; taking GLP-1 receptor agonists, finerenone, and other medications that have demonstrated a significant kidney protective effect; taking SGLT2 inhibitors less than 3 months before the renal biopsy. Patient information, including gender, age, diabetes duration, blood pressure, urinary albumin-to-creatinine ratio (ACR), estimate glomerular filtration rate (eGFR), glycated hemoglobin A1c (HbA1c), plasma lipid profile, medication history, images of PAS staining, Masson staining and transmission election microscopy results were retrospectively obtained from the hospital medical record system. The present study was conducted in accordance with the 1964 Helsinki ethical declaration and its subsequent amendments. The experimental design was approved by the Ethics Committee of the Third Affiliated Hospital of Sun Yat-sen University (approval number: II2024-05669).

Animal models

All experiments were approved by the Animal Ethics Committee of Sun Yat-sen University (approval number: IACUC-F3–22–0415, SYSU-IACUC-2020000006) and conducted in accordance with the standard protocols approved by the National Research Council's Guide for the Care and Use of Laboratory Animals and the Animal Ethics Committee of Sun Yat-sen University. All mice had free access to water and food, and were housed under a 12 h light/12 h dark cycle.

Seven-week-old male CD-1 mice were purchased from Guangdong Zhiyuan Biomedical Technology Co (Guangzhou, China). CD-1 mice were kept in a barrier environment at the Animal Experimental Center of the Third Affiliated Hospital of Sun Yat-sen University. After one week of adaptive feeding, CD-1 mice were randomly and blindly divided into two groups (n = 6 per group). The STZ-induced diabetic mouse model was constructed according to previously published study [23, 24]. In brief, the streptozotocin (STZ) group received an intraperitoneal injection of a single dose of STZ at 150 mg/kg in a citrate buffer (10 mM) to induce diabetes, while an equal volume of citrate buffer (10 mM) was injected in control group. Two weeks after STZ injection, mice with diabetes were confirmed by fasting blood glucose level greater than 16 mM. Eight weeks after diabetes induction, empagliflozin (10 mg/kg/day) dissolved in 0.5% hydroxypropyl methylcellulose (HPMC) or the same volume of 0.5% HPMC (control) was administered by oral gavage until ACR was significantly decreased (12 weeks) (n = 6 per group). Fasting blood glucose and body weight were measured every two weeks. The ACR was quantified by the Department of Laboratory Medicine of the Third Affiliated Hospital at Sun Yat-sen University.

Seven-week-old male C57BL/6 mice were obtained from GemPharmatech (Nanjing, China). After one week of adaptive feeding, C57BL/6 mice were randomly and blindly divided into two groups (n = 6 per group). The chow diet (CD) group were fed a diet containing 11% fat (Guangdong Medical Laboratory Animal Center, Guangzhou, China). The high-fat diet (HFD) group were fed a diet containing 58% fat (D12331, Research Diets, New Brunswick, NJ, USA) [24, 25]. DKD of C57BL/6 mice was confirmed by significantly elevated FBG, impaired glucose tolerance and increased ACR after 14 weeks of HFD-feeding. After 14 weeks of feeding, empagliflozin (10 mg/kg/day) or the same volume of 0.5% HPMC were administered via oral gavage until ACR was significantly decreased (6 weeks) (n = 6 per group). Fasting blood glucose and body weight were measured every two weeks. The plasma insulin level was detected by ELISA kits from Elabscience (Wuhan, China). The urinary albumin-to-creatinine ratio (ACR) was calculated by urinary microalbumin /urinary creatinine. The urinary albumin level and urinary creatinine level was determined using the creatinine companion and the Albuwell M kits purchased from Guangzhou Ruishu Biotechnology Co., Ltd (Guangzhou, China).

Seven-week-old B6·V-Lep^{ob}/J (*ob/ob*) mice were purchased from GemPharmatech (Nanjing, China) [26]. After one week of adaptive feeding, *ob/ob* mice were randomly divided into two groups (n = 6 per group) and fed a methionine- and choline-deficient (MCD) diet for 8 weeks. Mice were treated with empagliflozin (10 mg/kg/day) or an equal volume of 0.5% HPMC via oral gavage until ACR was significantly decreased (8 weeks).

After fasted overnight, the blood samples were collected from DKD mice anesthetized using isoflurane, followed by administration of more than 100 mg/kg of pentobarbital for euthanasia. Subsequently, mice were sacrificed through cervical vertebra dislocation, followed by tissue collection. The left kidneys from five mice in each group were cut in half longitudinally, and the half were then fixed in 4% formaldehyde for at least 24 h, embedded in paraffin and sectioned at 4–6 μm thickness for renal histological analysis, immunofluorescence, and immunochemistry.

Glucose and insulin tolerance test

The methods of intraperitoneal glucose tolerance test (IPGTT) and intraperitoneal insulin tolerance test (IPITT) were similar to those described in our previous study [27, 28]. In brief, after fasting for 6 h, mice were intraperitoneally injected with glucose (2 g/kg) solved in saline to perform an IPGTT. Blood samples were collected from the tail tip at 0, 30, 60 and 120 min after injection. Blood glucose was measured by a glucometer (ONETOUCH UltraVue, Johnson & Johnson, USA). An IPITT was performed by intraperitoneal injection of human insulin (0.65 IU/kg) (Novolin R, Novo Nordisk A/S, Copenhagen, Denmark) after 4 h of fasting.

Cell culture and treatment

Mycoplasma-free human immortalized RTPC (HK-2) (GNHu47, Cell Bank of the Chinese Academy of Sciences, Shanghai, China) were cultured in a 1:1 mixture of Dulbecco's Modified Eagle's Medium (DMEM) (GIBCO, Thermo Fisher Scientific, Waltham, MA, USA) and Ham's F12 medium (GIBCO, Thermo Fisher Scientific, Waltham, MA, USA) with 10% (v/v) fetal bovine serum (Procell, Wuhan, China). After starving in a serum-free medium for 12 h, HK-2 cells were synchronized and then treated with normal concentration of glucose (NG, 5.5 mM), high concentration of glucose (HG, 30 mM), or HG with empagliflozin (1 mM) for 72 h. For construction of

non-diabetic renal fibrosis model, HK-2 cells were treated with TGF-β (5 ng/ml) for 24 h, and then treated with empagliflozin (1 mM) for another 72 h.

Knockdown and overexpression of PKM2

The PKM2 shRNA and PKM2-overexpression vector (pcDNA3-PKM2, OE) were purchased from GenePharma (Shanghai GenePharma Co., Ltd., China) [29, 30]. HK-2 cells were transfected at 60%–65% confluence with PKM2 shRNA or overexpression vector by using Lipofectamine 3000 (Invitrogen, USA) according to the manufacturer's instructions [31]. For *PKM2* knockdown, the sequences of shRNA were cloned into pGPU6 vector. shPKM2: "5′-TTATTTGAGGAACTCCGCCGC-3". For transfection, cells were seeded into a 6-well plate, cultured overnight to 60–70% confluence, and then transfected using Lipofectamine 3000 reagent (Thermo Fisher Scientific, 11,668,019) supplemented with 2500 ng DNA or 50 nM (final concentration) siRNA [32].

Renal histopathology

Periodic acid-Schiff (PAS) staining and Masson trichrome staining were conducted according to previous published studies [33]. For PAS staining, the paraffin-embedded kidney slides were stained with 0.5% periodic acid for 10 min, washed, and stained again with Schiff reagent for 15 min. For Masson trichrome staining, the paraffin-embedded kidney sections were stained using Weigert's iron hematoxylin, azophloxine staining solution, phosphotungstic acid orange G, and light-green SF solution using a step-by-step method. After dehydration and xylene clearing, stained sections were observed under a light microscope (Olympus BX63; Olympus, Tokyo, Japan). Three photographs of each stained slide were taken.

Tubular injury was defined as tubular dilation, tubular atrophy, formation of cylindrical tubules, detachment of tubular epithelial cells or loss of brush border and thickening of the tubular basement membrane. The scoring system used was as follows: 0 points, no tubular damage; 1 point, < 10% renal tubular damage; 2 points; 10–25% renal tubular damage; 3 points, 25–50% renal tubular damage; 4 points, 50–74% renal tubular injury; 5 points, > 75% renal tubular injury damage [34].

Immunohistochemical analysis

Kidney sections from DKD patients, CD-1 mice and C57BL/6 mice were used for immunohistochemical staining. Immunohistochemical was carried out according to standard procedures reported in previous published studies[35, 36]. In brief, kidney tissues were fixed in 4% paraformaldehyde at 4 °C for 24 h, followed by dehydration by an ascending series of ethanol baths. Then the tissues were cleared with xylene and embedded in paraffin. The paraffin-embedded kidney tissues were cut into 4-μm sections. The kidney sections were then dewaxed with xylene and rehydrated with gradient ethanol. Specimens were incubated with 1% bovine serum albumin in PBS for 1 h and then incubated with the primary antibodies anti-neutrophil gelatinase associated lipocalin (NGAL) (1:500), anti-pyruvate kinase M2 (PKM2) (1:200), anti-E-cadherin (1:200), anti-Vimentin (1:200), anti-collagen type III α1 (COL3A1) (1:200), anti-α smooth muscle actin (αSMA) (1:200) primary antibodies at 4℃ overnight. Then the kidney sections were incubated with an enzyme-conjugated secondary antibody (1:2000) for 50 min at 37℃. The detailed antibody information is shown in Table 1 of the extra supplementary material (ESM).

Immunofluorescence staining

The initial immune-staining steps were performed as previously described [37, 38]. For kidney immunofluorescence staining, tissues were paraffin-embedded, de-paraffinized and rehydrated. Samples were incubated with primary antibodies for COL3A1 (1:200), PKM2 (1:200), and Lotus tetragonolobus lectin (LTL; 1:200) at 4 ℃ overnight, followed by incubation with fluorophore-conjugated secondary antibody (1:200) for 1 h at 37℃. Subsequently, 4,6-diamino-2-phenyl indole (DAPI) was applied for 5 min. For HK-2 cells immunofluorescence staining, cells were fixed in 4% paraformaldehyde for 30 min, and permeabilized with 0.5% Triton X-100 for 15 min. After that, the cells were blocked in 1% bovine serum albumin (BSA) for 1 h and incubated with the primary antibody for estrogen-related receptor α (ESRRA) (1:200) overnight at 4 ℃. Next, they were incubated with fluorophore-conjugated secondary antibody (1:10,000) for 1 h, followed by DAPI solution for 5 min at 37℃. Images were obtained using a Leica fluorescence microscope (Leica Microsystems, Wetzlar, Germany) at 200 × magnification. The detailed antibody information is shown in ESM Table 2.

RNA sequencing

HK-2 cells were seeded in six-well cultre plates and treated with NG, HG, or HG with empagliflozin for 72 h. Total RNA was isolated using TRIzol (#15,596,018, Invitrogen, Carlsbad, CA, USA). Each sample in NG, HG, and HG with empagliflozin groups were resultant mix of nine RNA extraction. According to the TruSeq™ RNA Sample Preparation Guide, paired-end libraries were synthesized used the TruSeq™ RNA Sample Prep Kit (Illumina, San Diego, CA, USA). Briefly, poly-A-containing mRNA molecules were purified using poly-T oligo-linked magnetic

Table 1 Clinical characteristics of the included patients

	DKD without EMPA (n=5)	DKD with EMPA (n=5)	*P* value
Gender			
Male	3 (60%)	3 (60%)	
Female	2 (40%)	2 (40%)	
Mean age (Years)	43 (33.5-57)	55 (51.5-56.5)	0.1508
Diabetes duration (Years)	13.00 (11.50-18.50)	11.00 (7.50-17.50)	0.3810
Medication duration (Years)	4.50 (3.75-5.50)	2.00 (1.50-2.50)	0.0079*
SBP (mmHg)	140.0 (127.5-156.5)	138.0 (121.0-187.0)	>0.9999
DBP (mmHg)	87.0 (80.0-98.5)	86.0 (75.5-107.5)	0.8413
UACR (mg/g)	7831 (6536-14376)	2682 (1248-5492)	0.0317*
eGFR (ml/min per 1.73m2)	20.89 (8.245-93.57)	49.94 (25.99-84.07)	0.8413
HbA1c (%)	6.70 (6.00-10.15)	7.90 (7.25-8.10)	0.7619
CHOL (mM)	5.060 (4.60-6.700)	5.210 (4.845-9.480)	0.6905
TG (mM)	2.990 (2.165-6.205)	2.240 (1.410-2.585)	0.1090
LDL (mM)	2.310 (1.960-3.960)	3.290 (2.680-5.440)	0.4206

beads and then fragmented into small pieces using divalent cations at 94ºC for 8 min. The cleaved RNA fragments were copied into first strand cDNA using reverse transcriptase and random primers. DNA Polymerase I and RNase H were used to synthesize second strand cDNA. These cDNA fragments went through an end repair process, the addition of a single 'A' base, and then ligation of the adapters. The products were then purified and enriched with PCR to create the final cDNA library. Purified libraries were quantified with a Qubit® 2.0 Fluorometer (Life Technologies, Carlsbad, CA, USA) and validated using an Agilent 2100 bioanalyzer (Agilent Technologies, Santa Clara, CA, USA) to confirm the insert size and calculate the mole concentration. Clusters were generated by cBot with the library diluted to 10 pM and then were sequenced on the Illumina NovaSeq 6000 (Illumina, San Diego, USA). The library construction and sequencing were performed by the Guangzhou Promegene Biotechnology Co., Ltd (Guangzhou, China). FPKM values were normalized per gene to obtain relative expression values.

Nuclear-cytosolic protein extraction

HK-2 cells were collected in ice-cold PBS (0.01 M) and then centrifuged at 800 RCF for 5 min. Tissue samples were cut into pieces and homogenized in the presence of phenylmethyl sulfonyl fluoride (PMSF). The samples were stored at -80 °C for subsequent western blot analysis. The cytoplasmic and nuclear protein fractions were separated using corresponding extraction reagents using a Nuclear

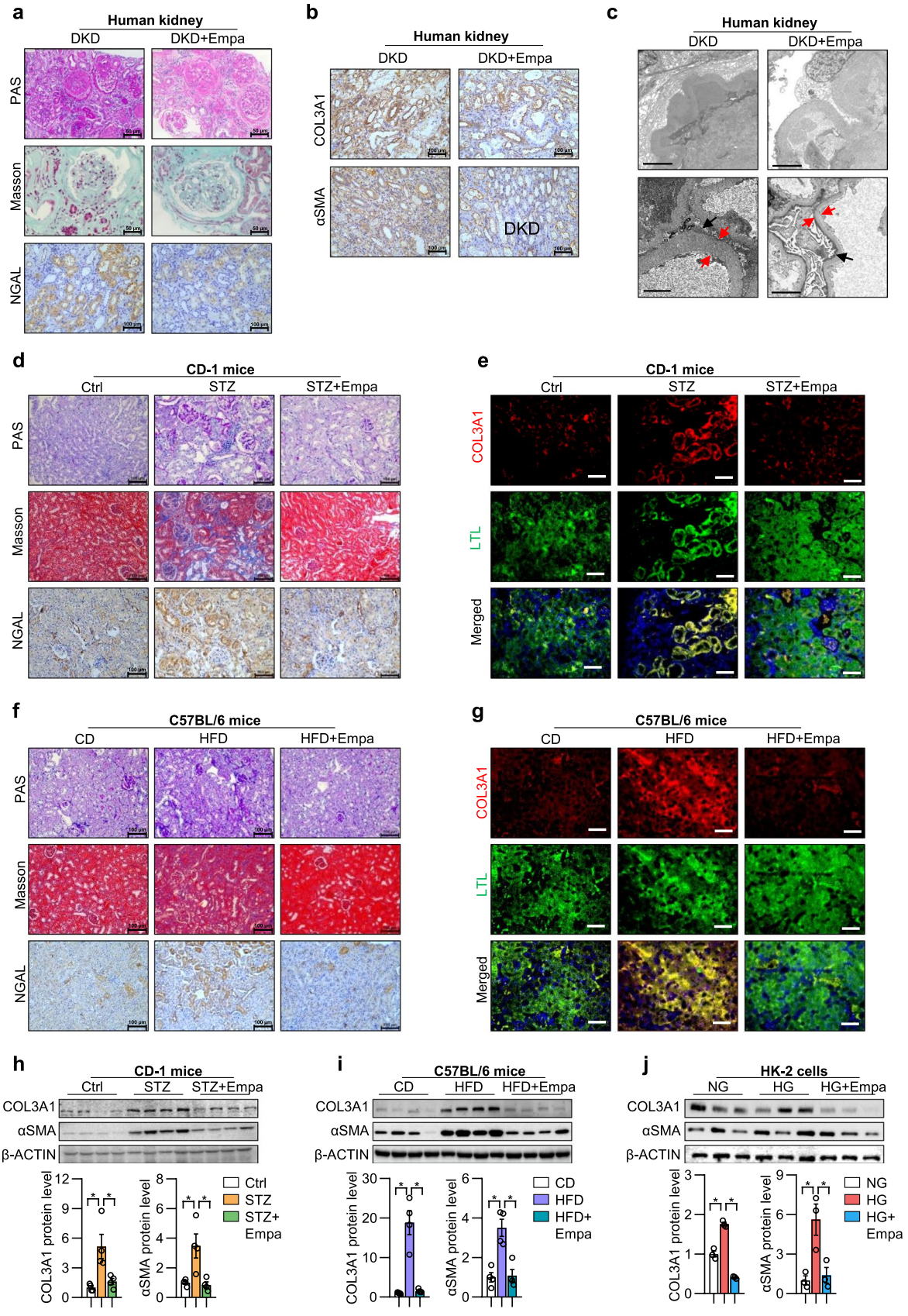
a
Human kidney
DKD
DKD+Empa
PAS
Masson
NGAL
b
Human kidney
DKD
DKD+Empa
COL3A1
αSMA
DKD
c
Human kidney
DKD
DKD+Empa
d
CD-1 mice
Ctrl
STZ
STZ+Empa
PAS
Masson
NGAL
e
CD-1 mice
Ctrl
STZ
STZ+Empa
COL3A1
LTL
Merged
f
C57BL/6 mice
CD
HFD
HFD+Empa
PAS
Masson
NGAL
g
C57BL/6 mice
CD
HFD
HFD+Empa
COL3A1
LTL
Merged
h
CD-1 mice
Ctrl
STZ
STZ+Empa
COL3A1
αSMA
β-ACTIN
COL3A1 protein level
αSMA protein level
Ctrl
STZ
STZ+ Empa
i
C57BL/6 mice
CD
HFD
HFD+Empa
COL3A1
αSMA
β-ACTIN
COL3A1 protein level
αSMA protein level
CD
HFD
HFD+ Empa
j
HK-2 cells
NG
HG
HG+Empa
COL3A1
αSMA
β-ACTIN
COL3A1 protein level
αSMA protein level
NG
HG
HG+ Empa

◂**Fig. 1** Empagliflozin ameliorate kidney fibrosis in DKD patients and DKD models **a** Representative images of PAS staining, Masson staining, and immunochemistry staining of NGAL from kidney sections of DKD patients. Images were obtained under a light microscope at 100X lens and 200X lens. **b** Representative images of immunochemistry staining of COL3A1 and αSMA from kidney sections of DKD patients. Images were obtained under a light microscope at 100X lens. **c** Representative kidney transmission electron microscopy (TEM) images of DKD patients. Thickened glomerular basement membrane was indicated by red arrow. Foot process effacement was indicated by black arrow. Scale bar, 2 μM. **d** Representative images of PAS staining, Masson staining, and immunochemistry staining of NGAL from kidney sections of CD-1 mice. Images were obtained under a light microscope at 100X lens. **e** Representative images of immunofluorescence staining for COL3A1 and Lotus tetragonolobus lectin (LTL) in CD-1 mice. Scale bar, 100 μm. **f** Representative images of PAS staining, Masson staining, and immunochemistry staining of NGAL from kidney sections of C57BL/6 mice. Images were obtained under a light microscope at 100X lens. **g** Representative images of immunofluorescence staining for COL3A1 and Lotus tetragonolobus lectin (LTL) in C57BL/6 mice. Scale bar, 100 μm. **h** Western blot analysis for collagen III α1 chain (COL3A1) and αSMA in the kidneys of CD-1 mice. For quantification, the band intensities of COL3A1 and αSMA protein were normalized to respective band intensities of β-actin. **i** Western blot analysis for COL3A1 and αSMA in the kidneys of C57BL/6 mice. For quantification, the band intensities of COL3A1 and αSMA protein were normalized to respective band intensities of β-actin. **j** Western blot analysis for COL3A1 and αSMA in the kidneys of HK-2 mice. For quantification, the band intensities of COL3A1 and αSMA protein were normalized to respective band intensities of β-actin. For all panels, $*p < 0.05$. *NG* normal glucose; *HG* high glucose, *HFD* high-fat diet, *EMPA* empagliflozin

and Cytoplasmic Protein Extraction Kit (#p0028; Beyotime Institute of Biotechnology, Shanghai, China) according to the manufacturer's protocol [39, 40]. Cytoplasmic protein and nuclear protein were separately collected and stored at -80 °C for western blot analysis.

Western blot

Western blot was performed according to previous published paper [26]. Kidney tissues and HK-2 cells were each homogenized in a lysis buffer containing protease and phosphatase inhibitors. Protein lysates were subjected to 8–10% polyacrylamide dodecyl sulfate gel electrophoresis (SDS-PAGE) and transferred onto polyvinylidene fluoride (PVDF) membranes. PVDF membranes were then incubated in primary antibodies against COL3A1 (1:1000), alpha smooth muscle actin (α-SMA;1:1000), PKM2 (1:1000), hexokinase 2 (HK2) (1:1000), phosphofructokinase (PFKP) (1:1000), ESRRA (1:1000), beta-actin (β-ACTIN; 1:1000), and Lamin B1 (1:1000) at 4 °C overnight. The membranes were then incubated with corresponding secondary antibodies (1:10,000) at 37 °C for 1 h. Band intensities were quantified using Image-j (NIH Bethesda, Maryland, USA). The detailed antibody information is shown in ESM Table 3.

Quantitative reverse transcription-PCR

Total RNA extracted from mice kidneys was converted to cDNA using a cDNA reverse transcription kit (Cat# RR047A, TAKARA, Kyoto, Japan) according to the manufacturer's instructions. Real-time quantitative PCR was performed using TB Green Premix Ex TaqII (Cat# RR820A, TAKARA, Kyoto, Japan) and conducted using a Light Cycler 480II Real-Time PCR System (Roche Diagnostics, Mannheim, Germany). β-actin was used as a housekeeping gene. The sequences of primers were listed in ESM Table 4.

Luciferase reporter assay

The JASPAR database (https://jaspar.genereg.net/) was used to identify the predicted ESSRA binding sites 2,000 base pairs (bp) upstream and 100 bp downstream of the transcription start site. The luciferase reporter assay was performed according to the previous published paper [37, 41]. The wild-type or mutant promoters of human *PKM2* were transduced into pGL3-basic vectors. The ESRRA expression plasmid, and wild-type or mutant pGL3-basic vectors were co-transfected into HEK 293 T cells (Dongze Biotech Co., Ltd, Guangdong, China). Subsequently, luciferase assays were performed on HEK 293 T cells at 70–80% confluence using a dual-luciferase reporter system (#E2940; Promega, Madison, WI, USA) according to the manufacturer's protocol.

Chromatin immunoprecipitation (ChIP)-qPCR

Chromatin immunoprecipitation (ChIP) assays were performed using a Chromatin Immunoprecipitation Kit (Millipore, Billerica, MA, USA) according to the instructions provided by the manufacturer [42, 43]. In brief, ESRRA antibody (Cell signaling technology, #13,826) was adopted for immunoprecipitation of chromatin, and IgG was negative control. Isolated RNA was assayed by RT-qPCR. Primers designed for the predicted binding site 1 of ESRRA at *PKM2* promoter regions were as follows: forward primer: 5'- CGGCGGAGGGATTGCG-3', reverse primer: 5'- GCT ACGCTGCAAAGACGAAGA-3'. Primers designed for the predicted binding site 2 of ESRRA at *PKM2* promoter regions were as follows: forward primer:5'- ACCGAAAGG GCAACCTGC-3', reverse primer: 5'- GGGCCGCCGCAA TCC-3'.

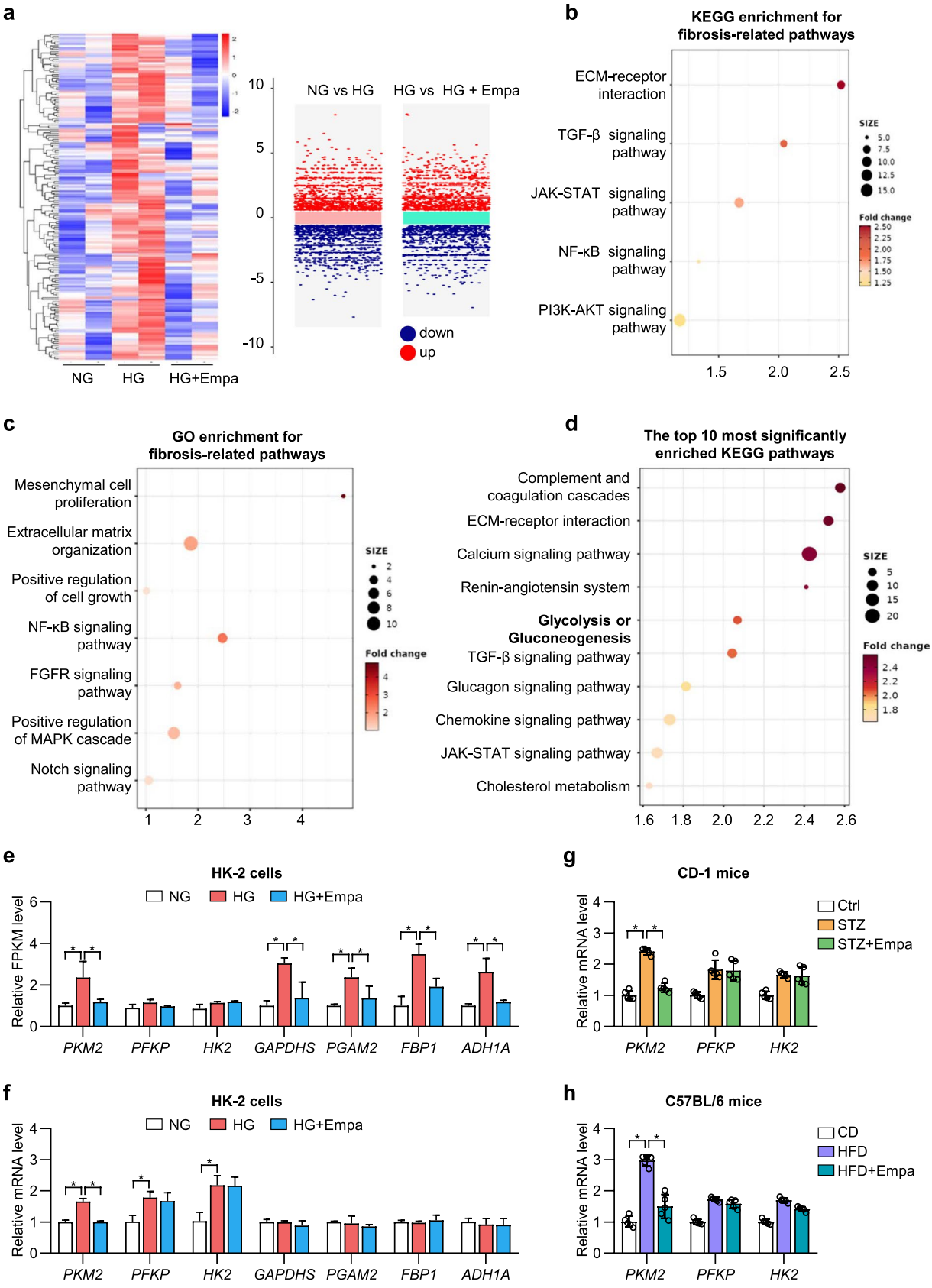
a
NG vs HG
HG vs HG + Empa
down
up
NG
HG
HG+Empa
b
KEGG enrichment for fibrosis-related pathways
ECM-receptor interaction
TGF-β signaling pathway
JAK-STAT signaling pathway
NF-κB signaling pathway
PI3K-AKT signaling pathway
SIZE
Fold change
c
GO enrichment for fibrosis-related pathways
Mesenchymal cell proliferation
Extracellular matrix organization
Positive regulation of cell growth
NF-κB signaling pathway
FGFR signaling pathway
Positive regulation of MAPK cascade
Notch signaling pathway
d
The top 10 most significantly enriched KEGG pathways
Complement and coagulation cascades
ECM-receptor interaction
Calcium signaling pathway
Renin-angiotensin system
Glycolysis or Gluconeogenesis
TGF-β signaling pathway
Glucagon signaling pathway
Chemokine signaling pathway
JAK-STAT signaling pathway
Cholesterol metabolism
e
HK-2 cells
NG
HG
HG+Empa
Relative FPKM level
PKM2
PFKP
HK2
GAPDHS
PGAM2
FBP1
ADH1A
g
CD-1 mice
Ctrl
STZ
STZ+Empa
Relative mRNA level
f
HK-2 cells
h
C57BL/6 mice
CD
HFD
HFD+Empa

◂**Fig. 2** Empagliflozin downregulated the mRNA level of *PKM2* in DKD **a** Heatmap and volcano map of the identified differentially expressed genes (DEGs) **b** Bubble chart of Kyoto Encyclopedia of Genes and Genomes (KEGG) enrichment for fibrosis-related pathways in Normal glucose (NG)-treated and high glucose (HG)-treated HK-2 cells. **c** Bubble chart of Gene Ontology (GO) enrichment for fibrosis-related pathways in Normal glucose (NG)-treated and high glucose (HG)-treated HK-2 cells. **d** KEGG analyses of enriched pathways upregulated in HG group and meanwhile downregulated by empagliflozin according to RNA-sequencing. **e** FPKM levels of glycolytic genes expression of glycolytic genes in HK-2 cells treated NG, HG or HG with empagliflozin according to RNA-sequencing. **f** Expression of glycolytic genes in HK-2 cells treated NG, HG or HG with empagliflozin analysed by RT-qPCR. **g** mRNA expression of *PKM2*, *PFKP*, and *HK2* in each CD-1 mouse group. **h** mRNA expression of *PKM2*, *PFKP*, and *HK2* in each C57BL/6 mouse group.For all panels, $*p < 0.05$. *NG*, normal glucose, *HG*, high glucose, *EMPA*, empagliflozin, *CD*, chow diet, *HFD*, high fat diet

Statistical analysis

All quantitative experiments were repeated at least 3 times independently. GraphPad Prism 8.0.1 was used for statistical analysis and creating graphs (GraphPad Software, San Diego, CA, USA). Data are expressed as the mean ± standard error of the mean (SEM). Comparisons between two groups were performed using the unpaired Student t-test. Comparisons between multiple groups were performed using one-way ANOVA, followed by Tukey's multiple comparisons test. Correlations were assessed using Spearman's rank correlation. Statistical significance was set at $P < 0.05$.

Results

SGLT2i ameliorate kidney fibrosis in DKD patients and DKD models

Patients without SGLT2i treatment were recruited into group 1, patients treated with SGLT2i were recruited into group 2. Clinical information on the patients is summarized in Table 1. The male to female ratios were both 3 to 2 in the two groups. There was no statistical difference in mean age, diabetes duration, systolic blood pressure, diastolic blood pressure, urinary creatine, eGFR, and glycated hemoglobin between the two patient groups (Table 1). The medication duration of group 1 was longer than in group 2 (Table 1). As expected, the urinary ACR was significantly lower in group 2 (Table 1). Extracellular matrix accumulation (PAS staining) and tubulointerstitial fibrosis (MASSON staining) were ameliorated in group 2 compared with group 1, indicating that SGLT2i treatment alleviated in DKD (Fig. 1A). The tubular injury marker NGAL were downregulated by empagliflozin (Fig. 1A). Fibrosis marker COL3A1 and αSMA were downregulated by empagliflozin in DKD patients (Fig. 1B, ESM Fig. 1A, B). Transmission electron microscopy (TEM) also showed the tubulointerstitial collagen deposition, basement thickening and foot process fusion were ameliorated by empagliflozin treatment (Fig. 1C).

After that, in vivo and in vitro experiments were carried out to confirmed the anti-fibrotic effect of empagliflozin. FBG and ACR were elevated in both STZ-treated CD-1 mice and HFD-treated C57BL/6 mice (ESM Fig. 1c–d, f–g). Body weight was reduced in STZ-treated CD1 mice (ESM Fig. 1e) and elevated in HFD-treated C57BL/6 mice (ESM Fig. 1h). Tubulointerstitial fibrosis were observed by PAS and MASSON staining in both of the two DKD mouse models (ESM Fig. 1i–j). Tubular injury score and NGAL were upregulated under STZ and HFD treatment (ESM Fig. 1k–n). Empagliflozin lowered FBG, improved body weight, and reduced ACR in both STZ-treated and HFD-treated mice (ESM Fig. 2a–h). Empagliflozin also lowered plasma insulin level, improved glucose tolerance (tested by IPGTT and IPITT) in HFD-treated mice (ESM Fig. 2I–K). Notably, empagliflozin significantly ameliorated tubular dilation, extracellular matrix accumulation (PAS staining), and tubulointerstitial fibrosis (MASSON staining) in both STZ-treated and HFD-treated mice (Fig. 1d, f). Tubular injury score and NGAL were also downregulated by empagliflozin (Fig. 1d, f, ESM Fig. 2l–o). Immunofluorescence and western blot were then used to detect fibrosis markers. Empagliflozin significantly downregulated COL3A1 and αSMA in both STZ-induced and HFD-induced DKD (Fig. 1e, g, h–i). In vitro experiments were carried out in HK-2 cells. Under HG condition, COL3A1 and αSMA were upregulated in HK-2 cells, while empagliflozin significantly downregulated these fibrosis makers (Fig. 1j).

Empagliflozin downregulated mRNA level of PKM2 in DKD

To investigate the mechanisms underlying the anti-fibrotic effect of empagliflozin, RNA sequencing was conducted in HK-2 cells (Fig. 2a). Both KEGG and GO analyses revealed that pathways associated with fibrosis were upregulated under HG conditions (Fig. 2b-c). Additionally, KEGG analysis was performed to identify the top ten enriched pathways that were upregulated in the HG group and simultaneously downregulated by empagliflozin. Differentially expressed genes were involved in cytokine-cytokine receptor interaction, calcium signaling, chemokine signaling, JAK-STAT signaling, TGF-beta signaling, glucagon signaling, glycolysis, starch and sucrose metabolism, renin-angiotensin system, and the pentose phosphate pathway (Fig. 3d). We focused our attention on differentially expressed genes involved in

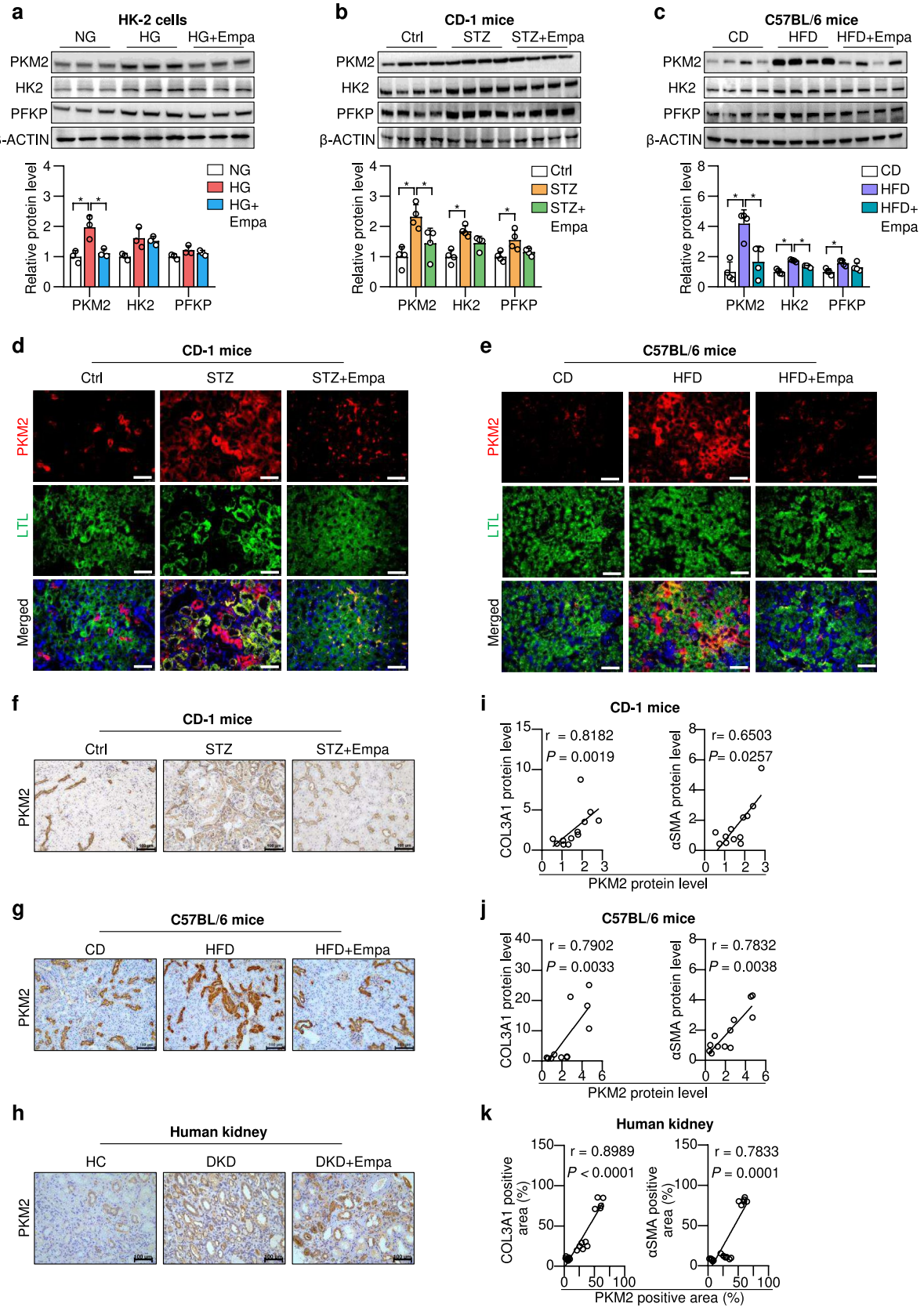
a
HK-2 cells
NG
HG
HG+Empa
PKM2
HK2
PFKP
β-ACTIN
Relative protein level
NG
HG
HG+ Empa
b
CD-1 mice
Ctrl
STZ
STZ+Empa
c
C57BL/6 mice
CD
HFD
HFD+Empa
d
e
LTL
Merged
f
g
h
Human kidney
HC
DKD
DKD+Empa
i
COL3A1 protein level
αSMA protein level
PKM2 protein level
r = 0.8182
P = 0.0019
r= 0.6503
P= 0.0257
j
r = 0.7902
P = 0.0033
r = 0.7832
P = 0.0038
k
COL3A1 positive area (%)
αSMA positive area (%)
PKM2 positive area (%)
r = 0.8989
P < 0.0001
r = 0.7833
P = 0.0001

◂**Fig. 3** Empagliflozin downregulated the protein level of PKM2 in DKD **a** Western blot analysis for PKM2 in HK-2 cells treated with NG, HG, or HG with empagliflozin. For quantification, the band intensities of PKM2 proteins were normalized to respective band intensities of β-ACTIN. **b** Western blot analysis for PKM2 in each group of CD-1 mice. For quantification, the band intensities of PKM2 proteins were normalized to respective band intensities of β-ACTIN. **c** Western blot analysis for PKM2 in each group of C57BL/6 mice. For quantification, the band intensities of PKM2 proteins were normalized to respective band intensities of β-ACTIN. **d–e** Representative images of immunofluorescence staining for PKM2 and Lotus tetragonolobus lectin (LTL) in CD-1 and C57BL/6 mice. Scale bar, 100 μm. **f** Representative images of immunochemistry staining of PKM2 from kidney sections of CD-1 mice. Images were obtained under a light microscope at 100X lens. **g** Representative images of immunochemistry staining of PKM2 from kidney sections of C57BL/6 mice. Images were obtained under a light microscope at 100X lens. **h** Representative images of immunochemistry staining of PKM2 from kidney sections of DKD patients. Images were obtained under a light microscope at 100X lens. **i–k** Correlation analysis of the expression of PKM2 protein levels with COL3A1 and αSMA in kidneys of DKD patients, each group of CD-1 mice and each group or C57BL/6 mice. For all panels, $*p < 0.05$. *NG* normal glucose, *HG* high glucose, *Ctrl* control, *CD* chow diet, *HFD* high-fat diet, *EMPA* empagliflozin

glycolysis, since the mechanisms by which empagliflozin reduces glycolysis have not yet been fully elucidated. RNA sequencing result showed that some of the genes involved in glycolytic pathway including PKM2, GAPDHS, PGAM2, FBP1, ADH1 were upregulated by HG and downregulated by empagliflozin. While other glycolytic genes including PFKP and HK2 showed no significant difference between NG, HG, and HG with empagliflozin group (Fig. 2e). The above glycolic genes in RNA sequencing were validated by RT-qPCR both in vitro. *PKM2, PFKP,* and *HK2* were upregulated by HG in HK-2 cells. Only PKM2 was downregulated by empagliflozin (Fig. 2f). The results were further validated in DKD mouse models. *PKM2* was upregulated by STZ and HFD, and was downregulated by empagliflozin (Fig. 2g, h).

Empagliflozin downregulated protein level of PKM2 in DKD

Genes fulfill their functions by being translated into functional proteins. In this study, we examined the protein expression levels of three key glycolytic enzymes: PKM2, HK2, and PFKP, in the context of diabetic kidney disease (DKD). Notably, PKM2 showed the highest level of upregulation under DKD conditions, while it was the most significantly downregulated enzyme in response to empagliflozin treatment (Fig. 3a–c). Immunofluorescence analysis revealed that in both the STZ and HFD groups, PKM2 was highly expressed and co-localized with LTL, a marker indicative of kidney proximal tubule cells. Notably, empagliflozin significantly downregulated PKM2 expression in both STZ-treated and HFD-treated mice (Fig. 3d–e). These findings were further corroborated by immunohistochemical analysis (Fig. 3f, g, ESM Fig. 2p, q). Importantly, PKM2 expression was found to be upregulated in the renal tubules of DKD patients, while it was downregulated in the empagliflozin-treated group (Fig. 3h, ESM Fig. 2r). Furthermore, a positive correlation was observed between PKM2 levels and the expression of fibrosis markers COL3A1 and αSMA in both DKD models and DKD patients (Fig. 3i–k).

Empagliflozin ameliorated renal fibrosis by downregulating PKM2 in vitro

To further elucidate whether empagliflozin ameliorates renal fibrosis via the downregulation of PKM2, we conducted experiments to overexpress and knock down PKM2 in HK-2 cells separately. The effects of overexpression and knockdown were validated through Western blot analysis (Fig. 4a–d). The PKM2 overexpression resulted in an elevation of fibrosis markers, including COL3A1 and αSMA (Fig. 4e–g). Importantly, the overexpression of PKM2 diminished the ameliorative effects of empagliflozin on renal fibrosis (Fig. 4h–k). Furthermore, PKM2 knockdown attenuated the downregulatory effects of empagliflozin on COL3A1 and αSMA, as evidenced by the comparison between the HG + shPKM2 and HG + shPKM2 + Empagliflozin groups (Fig. 4l–o).

Empagliflozin ameliorated EMT in DKD

Glycolysis plays a crucial role in the process of EMT. In this study, we examined the expression of the epithelial cell marker E-cadherin and the mesenchymal cell marker Vimentin in human kidney specimens as well as in kidney sections from DKD mouse models. Our findings revealed that E-cadherin was downregulated while Vimentin was upregulated in the renal tubular cells of DKD patients, STZ-treated mice, and HFD-treated mice (Fig. 5a–c). Notably, empagliflozin significantly ameliorated EMT in both DKD patients and DKD mouse models (Fig. 5a–c). Furthermore, the positive areas of E-cadherin were negatively correlated with the positive areas of PKM2. The positive areas of Vimentin were positively correlated with the areas of PKM2 (Fig. 5d–f).

Empagliflozin downregulated PKM2 by blocking the binding of ESRRA to the promoter

ESRRA, as a transcription factor, transferred into nucleus to activate downstream target genes. The nuclear translocation of ESRRA was increased in STZ-treated mice, HFD-fed

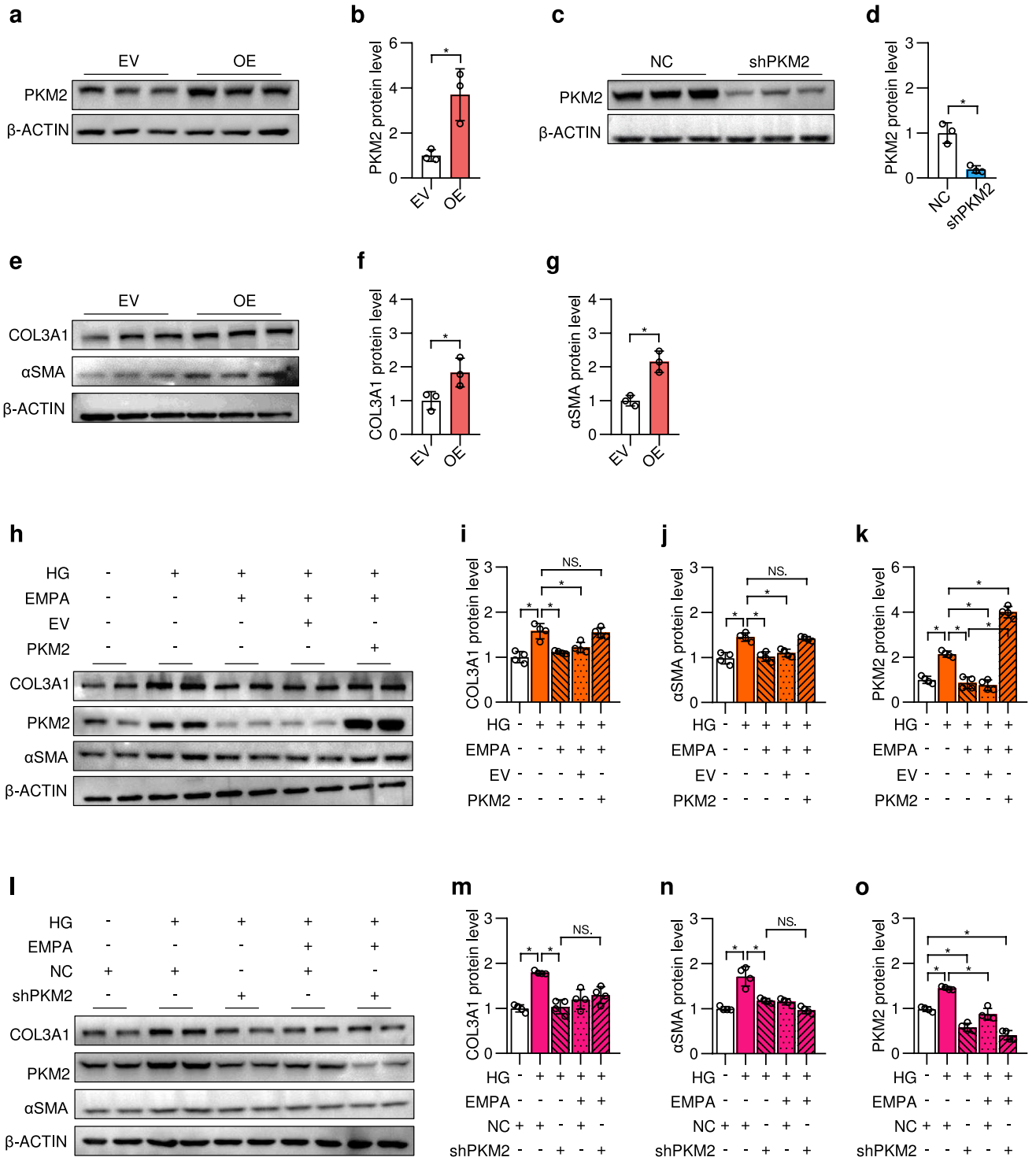

Fig. 4 Empagliflozin ameliorated renal fibrosis by downregulating PKM2 in vitro **a**–**b** Western blot analysis for PKM2 in HK-2 cells treated with empty vector or PKM2-overexpression plasmid (pcDNA3-PKM2). **c**–**d** Western blot analysis of PKM2 in HK-2 cells treated with shRNA-NC or shRNA-PKM2. **e**–**g** Western blot analysis of COL3A1 and αSMA in HK-2 cells treated with empty vector or pcDNA3-PKM2. **h**–**k** Western blot analysis of COL3A1, αSMA, and PKM2 in each group of HK-2 cells. **l**–**o** Western blot analysis of COL3A1, αSMA, and PKM2 in each group of HK-2 cells. For quantification, the band intensities of PKM2, COL3A1, and αSMA were normalized to respective band intensities of β-ACTIN

mice, and HG-treated HK-2 cells, and was decreased under empagliflozin treatment (Fig. 6a–d). The two predicted binding sites were further verified by dual-luciferase reporter gene assays. The mutation of either binding site 1 or binding site 2 significantly decreased the transcriptional activity of ESRRA (Fig. 6e). ChIP-qPCR analysis further indicated the enrichment of ESRRA at the PKM2 promoter (Fig. 6f). The results of ChIP-qPCR analysis also showed that the binding of ESRRA was upregulated by HG and was downregulated by empagliflozin at the two predicted binding sites (Fig. 6g).

Empagliflozin downregulated fibrosis markers in TGF-β-treated HK-2 cells

After stimulation of TGF-β, COL3A1 and αSMA were upregulated in HK-2 cells. Empagliflozin downregulated the fibrosis markers, indicating a direct amelioration effect of empagliflozin on renal fibrosis (ESM Fig. 2s).

Empagliflozin ameliorated kidney fibrosis and downregulated PKM2 in MCD treated ob/ob mice

In MCD diet-treated ob/ob (ob/MCD) mice, empagliflozin ameliorated renal tubular injury, as evidenced by PAS staining, and reduced tubulointerstitial fibrosis, as shown by Masson staining. It also suppressed the accumulation of NGAL and decreased the tubular injury score (ESM Fig. 3a–c). Additionally, COL3A1 and αSMA expression were downregulated by empagliflozin (ESM Fig. 3d, e). *Pkm2* was significantly downregulated by empagliflozin (ESM Fig. 3f). Western blot validated that PKM2 was the downregulated by empagliflozin, while empagliflozin showed no effect on HK2 and PFKP (ESM Fig. 3g). Immunofluorescence and immunochemistry results indicated that PKM2 was downregulated after empagliflozin treatment. Furthermore, E-cadherin was upregulated and Vimentin was downregulated in empagliflozin-treated group (ESM Fig. 3h–j). Empagliflozin decreased the nuclear translocation of ESRRA in ob/MCD mice (ESM Fig. 3k).

Discussion

The present study demonstrated that SGLT2 inhibitor empagliflozin can effectively alleviate EMT-related tubulointerstitial fibrosis by downregulating *PKM2* in DKD. The study showed that empagliflozin ameliorated kidney fibrosis in DKD patients and DKD models. *PKM2* was significantly upregulated in diabetic kidneys and HG-treated HK-2 cells. Empagliflozin downregulated *PKM2* and PKM2 in DKD models both in vivo and in vitro. Empagliflozin ameliorated renal fibrosis by reducing the recruitment of ESRRA to the *PKM2* promoter, thereby suppressing the transcription of *PKM2*.

The renal benefits of SGLT2 inhibitors have been validated in clinical trials [4–7]. RTPCs are the direct targets of SGLT2 inhibitors. Increasing evidence suggests that renal tubules play a critical role in the progression of DKD [44–48]. Large clinical trials have shown that SGLT2 inhibitors significantly reduce the risk of end-stage kidney disease in DKD patients. However, the outcomes of the above clinical trials mainly indicate the function of glomerulus [4–8]. The anti-fibrotic effect of SGLT2 inhibitors has been confirmed in several in vivo studies [9, 47, 49, 50]. Also, SGLT2 inhibitors have been reported to modulate multiple pathways implicated in renal fibrosis among DKD patients, potentially uncovering the mechanisms through which SGLT2 inhibition may ameliorate renal fibrosis [9–14]. Direct evidence that SGLT2 inhibitors improve renal fibrosis in DKD patients is yet to be fully established. In this study, we retrospectively analyzed renal biopsy results from DKD patients who were treated with SGLT2 inhibitors compared to those who were not. Staining techniques, including PAS staining and MASSON staining revealed that SGLT2 inhibitors reduced tubulointerstitial fibrosis in DKD patients. Transmission electron microscopy results show that empagliflozin improves renal interstitial collagen fiber proliferation, basement membrane thickening and foot process fusion in DKD patients. Furthermore, the anti-fibrotic effects of empagliflozin were validated in various DKD mouse models, including STZ-treated CD-1 mice, HFD-treated C57BL/6 mice, and MCD-treated *ob/ob* mice.

We then investigated the molecular mechanisms underlying empagliflozin-ameliorated-fibrosis. Although glucose metabolism is not the main energy supply method of renal tubules, key enzymes of glycolysis and gluconeogenesis still play some roles in renal tubular cells. Hexokinase, a key glycolytic enzyme, reduced mitochondrial membrane injury after metabolic stress [51]. Gluconeogenic enzymes including phosphoenolpyruvatecarboxykinase (PEPCK) and glucose-6-phosphatase (G6Pase) are highly expressed in the proximal tubules, making proximal tubules important in maintaining systemic glucose homeostasis [52–54]. In the present study, RNA sequencing analysis revealed that glycolysis pathway was significantly upregulated under HG condition and was downregulated by empagliflozin. SGLT2 inhibitors are reported to ameliorate glycolysis in metabolic disorders, including non-alcoholic fatty liver disease and DKD [41]. The progression of glycolysis depends on key glycolytic enzymes. However, the relationship between various glycolytic enzymes and the anti-fibrotic effects of SGLT2 inhibitors remains to be thoroughly investigated. Herein, *PKM2* exhibited the most significant elevation among glycolytic genes in HG-treated HK-2 cells. The upregulation of *Pkm2* was further confirmed

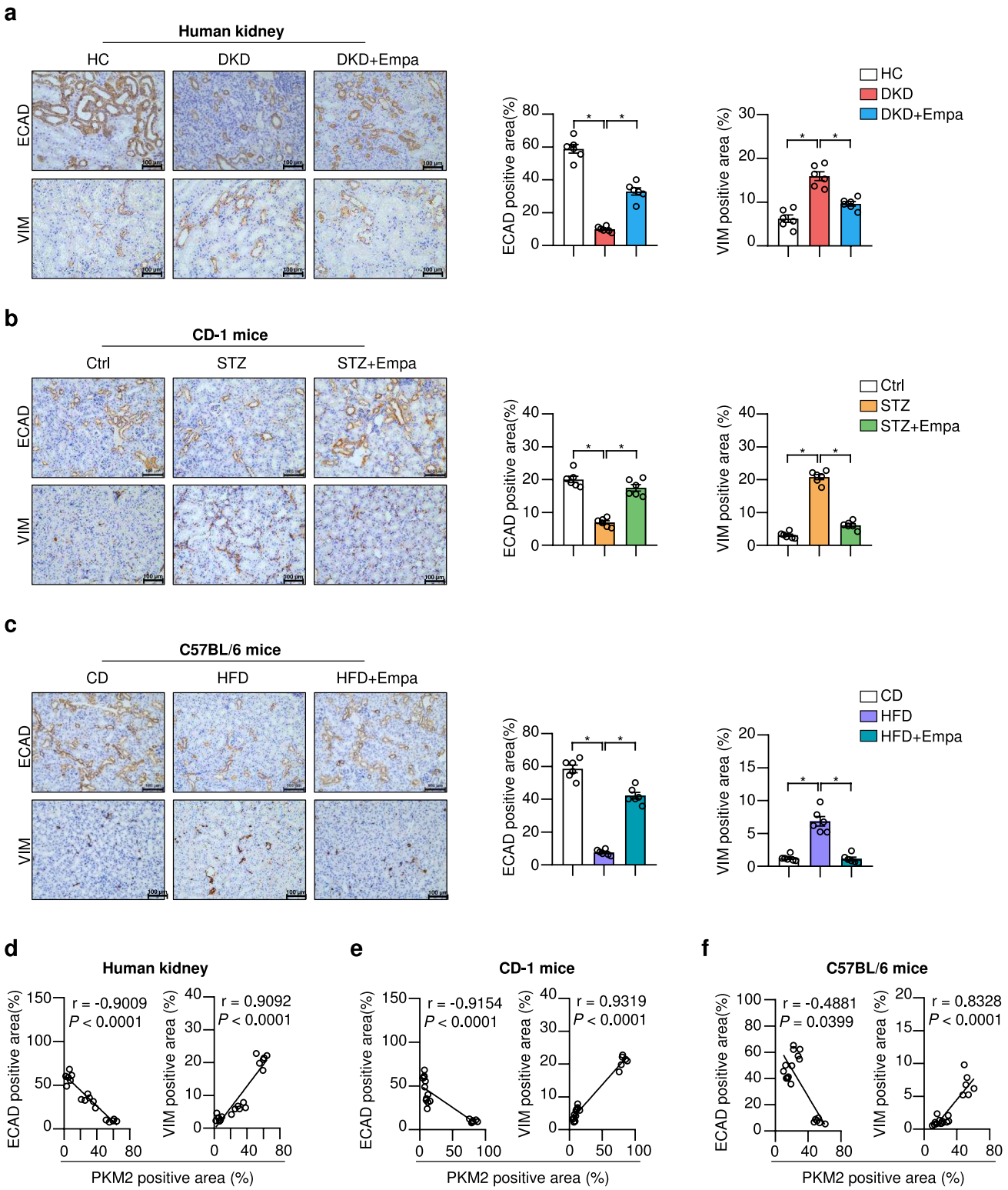

in DKD mouse models. The expression of *PKM2* was positively corelated with fibrosis markers COL3A1 and αSMA. Notably, empagliflozin downregulated *Pkm2* in both in vivo and in vitro DKD models. These findings suggest that *PKM2* is the key glycolytic gene involved in kidney fibrosis and the anti-fibrotic effect of empagliflozin in DKD.

PKM2 is translated from *PKM2*, serving as the rate-limiting enzyme of glycolysis [55]. In this study, we observed significant upregulation of PKM2 across various

◂**Fig. 5** Empagliflozin ameliorated EMT in DKD **a** Representative images of immunochemistry staining and the quantitative analysis of E-cadherin and Vimentin from kidney sections of DKD patients. Images were obtained under a light microscope at 100X lens. **b** Representative images of immunochemistry staining and the quantitative analysis of E-cadherin and Vimentin from kidney sections of each group of CD-1 mice. Images were obtained under a light microscope at 100X lens. **c** Representative images of immunochemistry staining and the quantitative analysis of E-cadherin and Vimentin from kidney sections of each group of C57BL/6 mice. Images were obtained under a light microscope at 100X lens. **e–f** Correlation analysis of the positive area of PKM2 with E-cadherin and Vimentin in kidneys of DKD patients, each group of CD-1 mice and C57BL/6 mice. For all panels, $*p < 0.05$. *Ctrl* control, *CD* chow diet, *HFD* high-fat diet, *NG* normal glucose, *HG* high glucose, *EMPA* empagliflozin, *ECAD* E-cadherin, *VIM* vimentin

DKD models. This upregulation was predominantly observed in RPTCs. Furthermore, the expression levels of PKM2 were also positively correlated with fibrosis markers, suggesting a critical role for PKM2 of RTPCs in kidney fibrosis. Empagliflozin effectively downregulated renal tubular PKM2. These findings further substantiate the role of PKM2 in inducing renal fibrosis, underscoring its significance in empagliflozin-ameliorated renal fibrosis.

Under normal condition, fatty acid oxidation is the main metabolic way in RTPCs. When glycolysis enhanced, the metabolic shift alters RTPCs identity and cell fate [56]. Transition to glycolysis state suppresses the normal epithelial phenotype and promotes a mesenchymal phenotype, leading to EMT [57]. This transition further stimulates the secretion of extracellular matrix components, including collagen and fibronectin, ultimately resulting in renal fibrosis [17, 58, 59]. Suppressing EMT in RTPCs may contribute to the anti-fibrotic effect of SGLT2 inhibitors. Thus, we then detected the EMT markers in the kidneys of DKD patients and DKD models. As expected, EMT was observed in the renal tubular cells in various DKD mouse models. Notably, empagliflozin effectively alleviated EMT. These findings underscore the anti-fibrotic effect of empagliflozin through the suppression of EMT in renal tubular cells.

Finally, we investigated the transcription factors responsible for *PKM2* upregulation. The transcription factors of PKM2 were predicted by UCSC (https://genome.ucsc.edu/index.html) and hTFtarget database (https://guolab.wchscu.cn/hTFtarget/). Among the predicted transcription factors, ESRRA has been rarely reported in DKD. As an orphan nuclear receptor, ESRRA regulates cell proliferation and cell metabolism by targeting various downstream genes. It is associated with various metabolic disorders, including obesity and non-alcoholic fatty liver disease [60–62]. Moreover, ESRRA is closely related with renal fibrosis induced by folic acid or unilateral ureteral obstruction [63]. However, there is little research focusing on the role of ESRRA in DKD. Herein, we found that ESRRA nuclear translocation was increased in DKD models both in vivo and in vitro and was significantly decreased by empagliflozin. Next, the binding sites of ESRRA at the *PKM2* promoter were predicted and confirmed. Empagliflozin downregulated *PKM2* via inhibiting the binding of ESRRA to *PKM2* promoter. These findings have further clarified the down-regulatory effect of SGLT2 inhibitors on PKM2 by elucidating the molecular mechanism.

To further validate the sufficient of PKM2 downregulation in the renal fibrosis amelioration mediated by empagliflozin, PKM2 was overexpressed and knocked down separately in HK-2 cells. Both overexpression and knockdown of PKM2 diminished the effect of empagliflozin on downregulation the fibrosis markers in HK-2 cells. These findings highlight the importance of PKM2 as a therapeutic target for DKD-related renal fibrosis.

In parallel to ongoing epidemics of obesity, The incidence of metabolic dysfunction-associated fatty liver disease (MAFLD) is increasing globally. Clinical trials indicate that the presence of MAFLD significantly increases the risk of end-stage kidney disease and renal fibrosis [64, 65]. However, the effect of SGLT2 inhibitors on renal fibrosis in MAFLD remains largely unclear. The MAFLD of ob/ob mice treated with methionine- and choline-deficient (MCD) diet used in the present study was confirmed in our previous published study [26]. Herein, renal fibrosis was observed in MCD-treated ob/ob mice. Furthermore, empagliflozin ameliorated renal fibrosis and EMT, downregulated PKM2 as well as reduced the nuclear translocation of ESRRA in the MAFLD mouse model.

To our knowledge, our study is the first to report the upregulation of renal tubular PKM2 and its downregulation induced by empagliflozin in patients with DKD. Other studies have analyzed the expression of PKM2 in podocytes from DKD patients. PKM2 was found to be downregulated in podocytes of DKD patients [66]. This disparity may arise from differing metabolic dependencies: tubular epithelial cells (TECs) rely predominantly on fatty acid β-oxidation, whereas podocytes are primarily dependent on glycolysis [46, 67]. In the context of DKD, glycolysis is observed to increase in TECs while decreasing in podocytes, which may explain the different trends of PKM2 in TECs and podocytes under diabetic condition [41, 68]. This study had a few limitations that must be considered. Firstly, the small number of patients included in our study could be considered a potential limitation. Many patients are reluctant to undergo renal biopsy due to its invasive nature and the associated risks of complications, including bleeding and infection. Secondly, the clinical information and pathology data of DKD patients were retrospectively collected, resulting in an inherent risk of recall bias and confounders (wash-out period absence). Thirdly, the *PKM2* tubules-specific

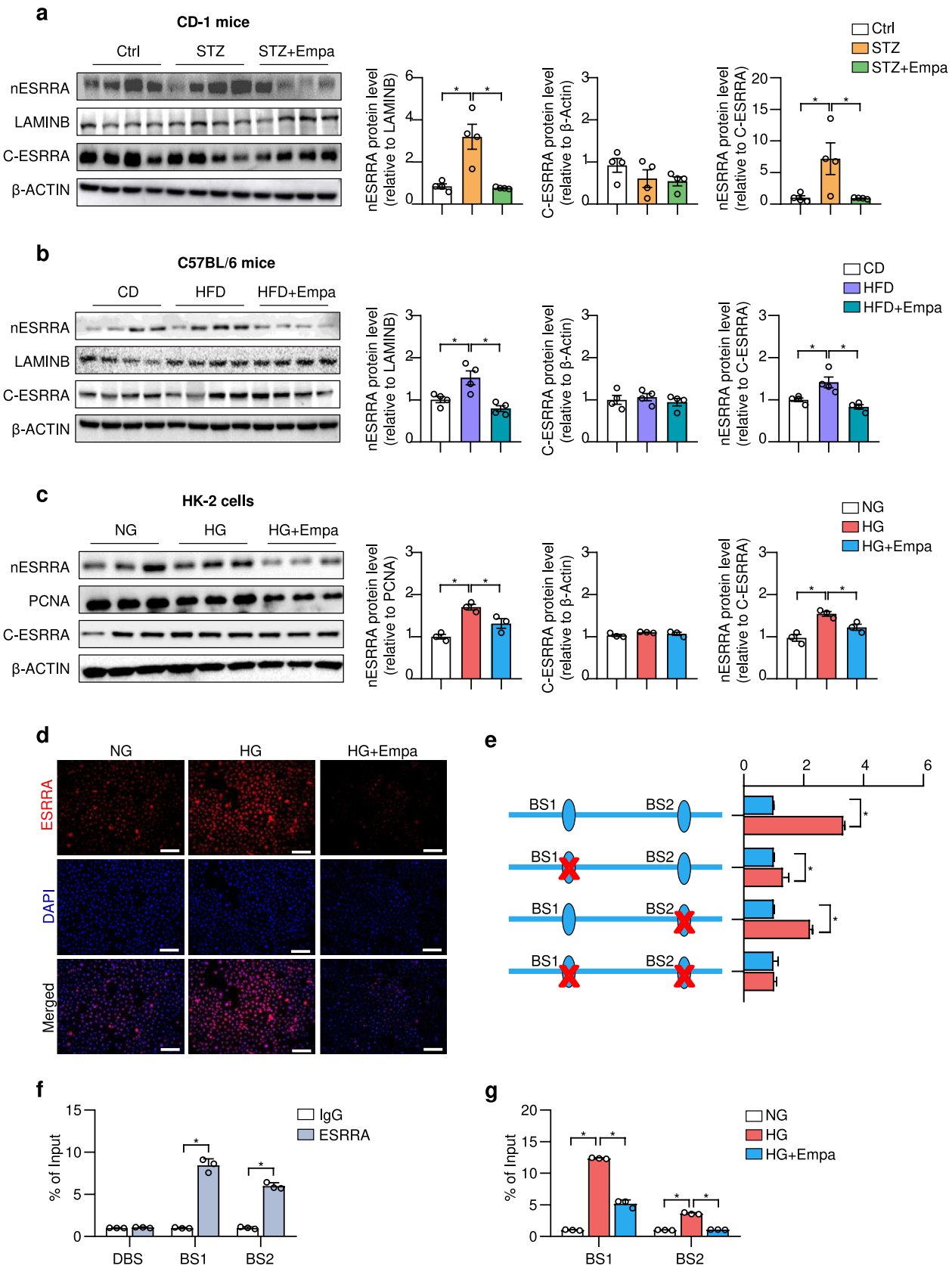
a
CD-1 mice
Ctrl
STZ
STZ+Empa
nESRRA
LAMINB
C-ESRRA
β-ACTIN
nESRRA protein level (relative to LAMINB)
C-ESRRA protein level (relative to β-Actin)
nESRRA protein level (relative to C-ESRRA)
b
C57BL/6 mice
CD
HFD
HFD+Empa
c
HK-2 cells
NG
HG
HG+Empa
PCNA
nESRRA protein level (relative to PCNA)
d
ESRRA
DAPI
Merged
e
BS1
BS2
f
IgG
ESRRA
% of Input
DBS
g

◂**Fig. 6** Empagliflozin downregulated *PKM2* by blocking the binding of estrogen-related receptor alpha (ESRRA) to the promoter **a** Western blot analysis for cytoplasmic and nuclear ESRRA in kidneys of each CD-1 mouse group. For quantification, the band intensities of cytoplasmic ESRRA were normalized to respective band intensities of β-ACTIN. The band intensities of nuclear ESRRA were normalized to respective band intensities of LAMIN-B. **b** Western blot analysis for cytoplasmic and nuclear ESRRA in kidneys of each C57BL/6 mouse group. For quantification, the band intensities of cytoplasmic ESRRA were normalized to respective band intensities of β-ACTIN. The band intensities of nuclear ESRRA were normalized to respective band intensities of LAMIN-B. **c** Western blot analysis for cytoplasmic and nuclear ESRRA in HK-2 cells treated with NG, HG, or HG with empagliflozin. For quantification, the band intensities of cytoplasmic ESRRA were normalized to respective band intensities of β-ACTIN. The band intensities of nuclear ESRRA were normalized to respective band intensities of PCNA. **d** Representative images of intracellular immunofluorescence staining for ESRRA in HK-2 cells treated with NG, HG, or HG with empagliflozin. Scale bar, 100 μm. **e** Luciferase reporter assays for the *PKM2* promoter were performed in HK-2 cells co-transfected with ESRRA expression plasmids and luciferase reporter plasmids containing wild-type or mutant mouse *PKM2* promoters. **f** ChIP analysis for ESRRA binding to the promoter of *PKM2* gene in HK-2 cells at different binding sites. **g** ChIP analysis for ESRRA binding to the promoter of *PKM2* gene in HK-2 cells treated with NG, HG, or HG with Empagliflozin at different binding sites. For all panels, $^{*}p < 0.05$. *STZ* streptozotocin, *CD* control diet, *HFD* high fat diet, *NG* normal glucose, *HG* high glucose, *EMPA* empagliflozin, *DBS* distant binding site, BS binding site

overexpression or knockdown mouse model is needed in the future study to further validate that the downregulation of PKM2 is sufficient to the attenuation of renal fibrosis by empagliflozin.

In conclusion, empagliflozin improves kidney fibrosis in DKD patients and DKD models. It ameliorates EMT of renal tubular cells through downregulating PKM2. At the molecular level, empagliflozin inhibits the transcription of *PKM2* by reducing the nuclear translocation of ESRRA and inhibiting its binding to the *PKM2* promoter. Our findings emphasize the significant role of PKM2 in both DKD-related kidney fibrosis and the amelioration of tubulointerstitial fibrosis mediated by empagliflozin.

Supplementary Information The online version contains supplementary material available at https://doi.org/10.1007/s00018-025-05688-8.

Author contributions Xiang Cai, Huanyi Cao, and Piaojian Yu carried out experiments, and wrote the manuscript. Meijun Wang and Hua liang contributed to data analysis. Xiaoqi Liang provided technical support with animal care. Fen Xu and Mengyin Cai contributed to the study design, data interpretation and revising the manuscript.

Funding National Natural Science Foundation of China,81670762,Mengyin Cai,82270942,Fen Xu,Natural Science Foundation of Guangdong Province,2020A1515011245,Mengyin Cai,2016A030313258,Mengyin Cai,Guangzhou Municipal Science and Technology Project,201707010118,Mengyin Cai

Data availability Original data are available upon reasonable request from the corresponding author.

Declarations

Conflict of interest The authors have no relevant financial or non-financial interests to disclose.

Ethical approval The retrospective study was approved by the Ethics Committee of the Third Affiliated Hospital of Sun Yat-sen University (approval number: II2024-056). Informed consent was obtained from all individual participants included in the study. All animal experiments were approved by the Animal Ethics Committee of the Third Affiliated Hospital of Sun Yat-sen University (approval number: IACUC-F3–22–0415, SYSU-IACUC-2020000006).

Consent to participate Informed consent was obtained from all individual participants included in the.

study.

References

1. Webster AC et al (2017) Chronic kidney disease. Lancet 389(10075):1238–1252
2. ElSayed NA et al (2023) 11. Chronic kidney disease and risk management: standards of care in diabetes-2023. Diabetes Care 46(Suppl 1):S191-s202
3. (2022) KDIGO 2022 Clinical practice guideline for diabetes management in chronic kidney disease. Kidney Disease: Improving Global Outcomes (KDIGO) Diabetes Work GroupKidney Int 102(5):S1–S127
4. Cherney DZI et al (2017) Effects of empagliflozin on the urinary albumin-to-creatinine ratio in patients with type 2 diabetes and established cardiovascular disease: an exploratory analysis from the EMPA-REG OUTCOME randomised, placebo-controlled trial. Lancet Diabetes Endocrinol 5(8):610–621
5. Wanner C et al (2016) Empagliflozin and Progression of Kidney Disease in Type 2 Diabetes. N Engl J Med 375(4):323–334
6. Perkovic V et al (2019) Canagliflozin and Renal Outcomes in Type 2 Diabetes and Nephropathy. N Engl J Med 380(24):2295–2306
7. Wiviott SD et al (2019) Dapagliflozin and cardiovascular outcomes in type 2 diabetes. N Engl J Med 380(4):347–357
8. Herrington WG et al (2023) Empagliflozin in patients with chronic kidney disease. N Engl J Med 388(2):117–127
9. Heerspink HJL et al (2019) Canagliflozin reduces inflammation and fibrosis biomarkers: a potential mechanism of action for

beneficial effects of SGLT2 inhibitors in diabetic kidney disease. Diabetologia 62(7):1154–1166
10. Llorens-Cebrià C et al (2022) Antioxidant roles of SGLT2 inhibitors in the kidney. Biomolecules 12(1):143
11. Nabrdalik-Leśniak D et al (2021) Influence of SGLT2 inhibitor treatment on urine antioxidant status in type 2 diabetic patients: a pilot study. Oxid Med Cell Longev 2021:5593589
12. van Bommel EJM et al (2020) The renal hemodynamic effects of the SGLT2 inhibitor dapagliflozin are caused by post-glomerular vasodilatation rather than pre-glomerular vasoconstriction in metformin-treated patients with type 2 diabetes in the randomized, double-blind RED trial. Kidney Int 97(1):202–212
13. Kim SR et al (2020) SGLT2 inhibition modulates NLRP3 inflammasome activity via ketones and insulin in diabetes with cardiovascular disease. Nat Commun 11(1):2127
14. Sunilkumar S et al (2025) REDD1 expression in podocytes facilitates renal inflammation and pyroptosis in streptozotocin-induced diabetic nephropathy. Cell Death Dis 16(1):79
15. Liu X et al (2020) Tubule-derived exosomes play a central role in fibroblast activation and kidney fibrosis. Kidney Int 97(6):1181–1195
16. Liu BC et al (2018) Renal tubule injury: a driving force toward chronic kidney disease. Kidney Int 93(3):568–579
17. Lovisa S et al (2015) Epithelial-to-mesenchymal transition induces cell cycle arrest and parenchymal damage in renal fibrosis. Nat Med 21(9):998–1009
18. Thiery JP, Sleeman JP (2006) Complex networks orchestrate epithelial-mesenchymal transitions. Nat Rev Mol Cell Biol 7(2):131–142
19. Thiery JP et al (2009) Epithelial-mesenchymal transitions in development and disease. Cell 139(5):871–890
20. Huang R, Fu P, Ma L (2023) Kidney fibrosis: from mechanisms to therapeutic medicines. Signal Transduct Target Ther 8(1):129
21. Yang L et al (2010) Epithelial cell cycle arrest in G2/M mediates kidney fibrosis after injury. Nat Med 16(5):535–543
22. Thomas K et al (2022) Glutamine prevents acute kidney injury by modulating oxidative stress and apoptosis in tubular epithelial cells. JCI Insight. https://doi.org/10.1172/jci.insight.163161
23. Xu Z et al (2021) METTL14-regulated PI3K/Akt signaling pathway via PTEN affects HDAC5-mediated epithelial-mesenchymal transition of renal tubular cells in diabetic kidney disease. Cell Death Dis 12(1):32
24. Urabe H et al (2016) Ablation of a small subpopulation of diabetes-specific bone marrow-derived cells in mice protects against diabetic neuropathy. Am J Physiol Endocrinol Metab 310(4):E269–E275
25. Müller TD et al (2013) p62 links β-adrenergic input to mitochondrial function and thermogenesis. J Clin Invest 123(1):469–478
26. Shen Y et al (2023) SGLT2 inhibitor empagliflozin downregulates miRNA-34a-5p and targets GREM2 to inactivate hepatic stellate cells and ameliorate non-alcoholic fatty liver disease-associated fibrosis. Metabolism 146:155657
27. Cao H et al (2023) Malonylation of Acetyl-CoA carboxylase 1 promotes hepatic steatosis and is attenuated by ketogenic diet in NAFLD. Cell Rep 42(4):112319
28. Zheng X et al (2017) SIRT1/HSF1/HSP pathway is essential for exenatide-alleviated, lipid-induced hepatic endoplasmic reticulum stress. Hepatology 66(3):809–824
29. Wang Q et al (2022) Suppression of osteoclast multinucleation via a posttranscriptional regulation-based spatiotemporally selective delivery system. Sci Adv 8(26):eabn3333
30. Hu Y et al (2022) Demethylase ALKBH5 suppresses invasion of gastric cancer via PKMYT1 m6A modification. Mol Cancer 21(1):34
31. Bai Y et al (2024) Marrow mesenchymal stem cell mediates diabetic nephropathy progression via modulation of Smad2/3/WTAP/m6A/ENO1 axis. Faseb j 38(11):e23729
32. Wu J et al (2021) APOL1 risk variants in individuals of African genetic ancestry drive endothelial cell defects that exacerbate sepsis. Immunity 54(11):2632-2649.e6
33. Chen JH et al (2022) The down-regulation of XBP1, an unfolded protein response effector, promotes acute kidney injury to chronic kidney disease transition. J Biomed Sci 29(1):46
34. Xu S et al (2022) Bone marrow mesenchymal stem cell-derived exosomal miR-21a-5p alleviates renal fibrosis by attenuating glycolysis by targeting PFKM. Cell Death Dis 13(10):876
35. Ju B et al (2009) Co-activation of hedgehog and AKT pathways promote tumorigenesis in zebrafish. Mol Cancer 8:40
36. Liu Y et al (2022) Nrf2 deficiency deteriorates diabetic kidney disease in Akita model mice. Redox Biol 58:102525
37. Wang MJ et al (2023) SIRT1-dependent deacetylation of Txnip H3K9ac is critical for exenatide-improved diabetic kidney disease. Biomed Pharmacother 167:115515
38. Lu YH et al (2020) Empagliflozin attenuates hyperuricemia by upregulation of ABCG2 via AMPK/AKT/CREB signaling pathway in type 2 diabetic mice. Int J Biol Sci 16(3):529–542
39. Huang X et al (2018) Targeting epigenetic crosstalk as a therapeutic strategy for EZH2-aberrant solid tumors. Cell 175(1):186-199.e19
40. Lou F et al (2020) Excessive polyamine generation in keratinocytes promotes self-RNA sensing by dendritic cells in psoriasis. Immunity 53(1):204-216.e10
41. Cai T et al (2020) Sodium-glucose cotransporter 2 inhibition suppresses HIF-1α-mediated metabolic switch from lipid oxidation to glycolysis in kidney tubule cells of diabetic mice. Cell Death Dis 11(5):390
42. Xing S et al (2021) Hypoxia downregulated miR-4521 suppresses gastric carcinoma progression through regulation of IGF2 and FOXM1. Mol Cancer 20(1):9
43. Hong S, Zheng G, Wiley JW (2015) Epigenetic regulation of genes that modulate chronic stress-induced visceral pain in the peripheral nervous system. Gastroenterology 148(1):148-157.e7
44. Zeni L et al (2017) A more tubulocentric view of diabetic kidney disease. J Nephrol 30(6):701–717
45. Di Vincenzo A et al (2020) Renal structure in type 2 diabetes: facts and misconceptions. J Nephrol 33(5):901–907
46. Kang HM et al (2015) Defective fatty acid oxidation in renal tubular epithelial cells has a key role in kidney fibrosis development. Nat Med 21(1):37–46
47. Vallon V, Thomson SC (2020) The tubular hypothesis of nephron filtration and diabetic kidney disease. Nat Rev Nephrol 16(6):317–336
48. Doke T, Susztak K (2022) The multifaceted role of kidney tubule mitochondrial dysfunction in kidney disease development. Trends Cell Biol 32(10):841–853
49. Kogot-Levin A et al (2020) Proximal tubule mTORC1 Is a central player in the pathophysiology of diabetic nephropathy and its correction by SGLT2 inhibitors. Cell Rep 32(4):107954
50. Zhang Y et al (2018) A sodium-glucose cotransporter 2 inhibitor attenuates renal capillary injury and fibrosis by a vascular endothelial growth factor-dependent pathway after renal injury in mice. Kidney Int 94(3):524–535
51. Gall JM et al (2011) Hexokinase regulates Bax-mediated mitochondrial membrane injury following ischemic stress. Kidney Int 79(11):1207–1216
52. Pollock AS (1989) Induction of renal phosphoenolpyruvate carboxykinase mRNA: suppressive effect of glucose. Am J Physiol 257(1 Pt 2):F145–F151

53. Mithieux G, Rajas F, Gautier-Stein A (2004) A novel role for glucose 6-phosphatase in the small intestine in the control of glucose homeostasis. J Biol Chem 279(43):44231–44234
54. Sasaki M et al (2017) Dual regulation of gluconeogenesis by insulin and glucose in the proximal tubules of the kidney. Diabetes 66(9):2339–2350
55. Christofk HR et al (2008) The M2 splice isoform of pyruvate kinase is important for cancer metabolism and tumour growth. Nature 452(7184):230–233
56. Zhu Z et al (2022) Transition of acute kidney injury to chronic kidney disease: role of metabolic reprogramming. Metabolism 131:155194
57. Srivastava SP et al (2018) SIRT3 deficiency leads to induction of abnormal glycolysis in diabetic kidney with fibrosis. Cell Death Dis 9(10):997
58. Zhou D, Liu Y (2016) Renal fibrosis in 2015: understanding the mechanisms of kidney fibrosis. Nat Rev Nephrol 12(2):68–70
59. Djudjaj S, Boor P (2019) Cellular and molecular mechanisms of kidney fibrosis. Mol Aspects Med 65:16–36
60. B'Chir W et al (2018) Divergent role of estrogen-related receptor α in lipid- and fasting-induced hepatic steatosis in mice. Endocrinology 159(5):2153–2164
61. Chen CY et al (2021) Inhibition of estrogen-related receptor α blocks liver steatosis and steatohepatitis and attenuates triglyceride biosynthesis. Am J Pathol 191(7):1240–1254
62. Yang M et al (2020) Dysfunction of estrogen-related receptor alpha-dependent hepatic VLDL secretion contributes to sex disparity in NAFLD/NASH development. Theranostics 10(24):10874–10891
63. Dhillon P et al (2021) The nuclear receptor ESRRA protects from kidney disease by coupling metabolism and differentiation. Cell Metab 33(2):379-394.e8
64. Zhao L et al (2024) Impact of non-alcoholic fatty liver disease and fibrosis on mortality and kidney outcomes in patients with type 2 diabetes and chronic kidney disease: a multi-cohort longitudinal study. Diabetes Obes Metab 26(10):4241–4250
65. Musso G et al (2014) Association of non-alcoholic fatty liver disease with chronic kidney disease: a systematic review and meta-analysis. PLoS Med 11(7):e1001680
66. Chen Z et al (2023) Reduction of anaerobic glycolysis contributes to angiotensin II-induced podocyte injury with foot process effacement. Kidney Int 103(4):735–748
67. Ozawa S et al (2015) Glycolysis, but not Mitochondria, responsible for intracellular ATP distribution in cortical area of podocytes. Sci Rep 5:18575
68. Yuan Q et al (2020) Role of pyruvate kinase M2-mediated metabolic reprogramming during podocyte differentiation. Cell Death Dis 11(5):355